Cluster Spin Glass Formation in the Double Double Perovskite CaMnFeTaO6

Cluster spin glass formation in the double double perovskite $CaMnFeTaO_6$

Padraig Kearins,[†] Elena Solana-Madruga,[†] Kunlang Ji[†] , Clemens Ritter,[‡] and J. Paul Attfield*[†]

[†]Centre for Science at Extreme Conditions (CSEC) and School of Chemistry, University of Edinburgh, Peter Guthrie Tait Road, Edinburgh EH9 3FD (UK)

[‡] Institut Laue-Langevin, 38042 Grenoble Cedex, France.

* Email; j.p.attfield@ed.ac.uk

Abstract: $CaMnFeTaO_6$ has been synthesised at 1200 °C under 10 GPa pressure. Powder neutron diffraction shows that $CaMnFeTaO_6$ adopts a double double perovskite structure (tetragonal space group $P4_2/n$, lattice parameters a = 7.683(3) and c = 7.685(7) Å) with cation disorder at all transition metal sites. Magnetization measurements reveal an apparent ferro- or ferri-magnetic transition at T_{m1} = 51 K and a susceptibility peak at T_{m2} = 20 K, but no long-range magnetic order is observed by neutron diffraction down to 1.5 K. This is attributed to formation of superparamagnetic clusters of ferrimagnetically ordered spins below T_{m1} that freeze into a cluster spin glass at $T_f = T_{m2}$. AC magnetisation measurements confirm the cluster spin glass ground state. Disorder from substitution of Fe^{2+} for Mn^{2+} and Fe^{3+}/Ta^{5+} inversion disrupts the network of superexchange interactions leading to the cluster spin glass ground state, in contrast to other $P4_2/n$ double double perovskites where long range magnetic order is stabilised.

Introduction

The ABO_3 perovskite structure is known to accept a wide range of different cations onto the A- and B-sites, and also for the ability to order multiple cations, giving rise to double perovskites $AA'B_2O_6$ or $A_2BB'O_6$.[1,2] Cation ordering gives rise to ferrimagnetism and half metallicity in the $A_2BB'O_6$ family with rocksalt-type B-cation order, notably in Sr_2FeMoO_6.[3,4] In recent years, high pressure synthesis has been used to prepare analogous double perovskites in which magnetic Mn^{2+} replaces non-magnetic A-site cations like Sr^{2+}, giving rise to further ferrimagnetic materials such as Mn_2FeReO_6,[5,6] and Mn_2MReO_6 analogs (M = Mn, Co, Ni)[7,8,9] which display complex low temperature antiferromagnetic orders. This high pressure synthetic research also led to discovery of a new $AA'BB'O_6$ double double perovskite structure with tetragonal space group $P4_2/n$, which is doubly cation ordered with columnar A-site order and rocksalt B-ordering. This was first reported for $MnRMnSbO_6$ (R = rare earth)[10,11] and subsequently for $CaMnMReO_6$ (B = Mn, Fe, Co, Ni)[12,13,14] phases.

The $P4_2/n$ double double perovskite structure is notable for having five different cation sites as two inequivalent positions (with tetrahedral and square-planar coordination) are formed within the A-site Mn^{2+} columns. Magnetic couplings between the multiple spin sublattices give rise to complex magnetic orders. $Mn\mathit{R}MnSbO_6$ perovskites display two ferromagnetic sublattices at the two Mn sites in the structure which are antiferromagnetically coupled to each other with magnetic ordering temperatures ranging from 46 to 76 K.[10,11] $CaMnFeReO_6$ shows antiparallel Fe^{3+}/Re^{5+} ferrimagnetic ordering at 500 K and a second ferrimagnetic ordering of the opposed inequivalent tetrahedral and square-planar A-site Mn^{2+} at 70 K.[12,13] $CaMnMnReO_6$ displays antiferromagnetic B-site spin ordering at 120 K, but ferromagnetic ordering of the A-site spins at 100 K.[12] $CaMnCoReO_6$ orders ferrimagnetically below Curie temperature T_C = 188 K and $CaMnNiReO_6$ is a rare example of an insulating ferromagnetic perovskite oxide where all four distinct spin sublattices are collinearly ordered below T_C = 152 K.[14] All of these previously studied double double perovskites have displayed long range magnetic order at low temperatures. In this paper, we report a new double double perovskite $CaMnFeTaO_6$ that is notable for not forming a long-range spin order below apparent magnetic transitions, and a cluster spin glass ground state is proposed.

Experimental

$CaMnFeTaO_6$ was synthesised under high pressure and high temperature conditions by mixing stoichiometric amounts of $Ca_2Fe_2O_5$, MnO and Ta_2O_5. $Ca_2Fe_2O_5$ was prepared by mixing stoichiometric proportions of $CaCO_3$ and Fe_2O_3 and heating at 1200 ° under a N_2 flow. The $CaMnFeTaO_6$ precursor mixture was packed into a Pt capsule and compressed to 10 GPa using a Walker-type multi-anvil press. The sample was heated over 10 minutes to 1200 °C, held at this temperature for 20 minutes before quenching to room temperature, after which the pressure was slowly released. Powder X-ray diffraction was used to confirm that a single phase perovskite sample was formed.

Neutron powder diffraction data from a ~50 mg sample were collected on the D20 beamline at the Institut Laue-Langevin, Grenoble. Data were analysed using the

Fullprof suite.[15] Magnetisation measurements were made using a PPMS Quantum Design magnetometer.

Results and Discussion

The crystal structure of $CaMnFeTaO_6$ was analysed by fitting 300 K neutron powder diffraction data with wavelength λ = 1.54 Å. The Rietveld fit (Figure 1) confirms that $CaMnFeTaO_6$ adopts the above $P4_2/n$ double double perovskite structure in tetragonal space group. The lattice parameters were refined to be a = 7.683(3) and c = 7.685(7) Å. The high contrast between neutron scattering lengths of the three transition metals present; Mn (-3.73 fm), Fe (9.45 fm) and Ta (6.91 fm);[16] allowed their proportions at each site to be refined. The use of a single dataset without other contrast information, e.g. from resonant X-ray data, only enables two elements to be refined at each site. However, an extensive combined neutron and resonant X-ray study of cation disorder in an oxide of comparable complexity - the $Tl_{0.5}Pb_{0.5}Sr_2Ca_2Cu_3O_9$ superconductor - showed that only one type of doping at each site was favored, e.g. Ca was specifically substituted by Tl rather than by Pb or Sr.[17] This likely indicates that while all dopants would lead to similar increases in lattice entropy, cross-substitution of one dopant is enthalpically favored in complex oxides.

A substantial amount of disorder was discovered in $CaMnFeTaO_6$ as shown by the results in Table 1. The Ca-site within the A-cation columns is fully occupied, but the tetrahedral A1 and square-planar A2 sites that alternate along the columns of Mn were found to contain 12(4)% and 24(1)% Fe respectively. The preference of Fe^{2+} for the square-planar environment likely reflects crystal field effects - Fe^{2+} is found in this environment in the reduced oxide $SrFeO_2$.[18] 18(3)% Fe/Ta antisite disorder between the B/B'-cation positions was also observed. The refined composition of $CaMn_{0.82}Fe_{1.18}TaO_6$ is thus Fe-rich and Mn-poor relative to the ideal stoichiometry. The refined crystal structure is shown in Figure 2.

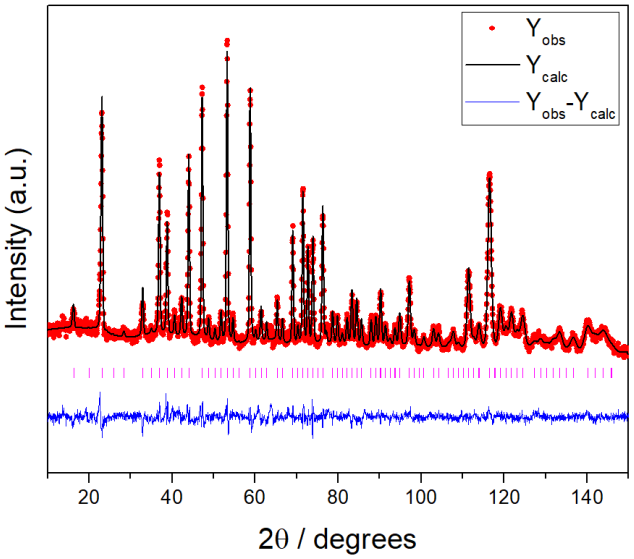

Figure 1: Rietveld fit to 300 K powder neutron diffraction data for $CaMnFeTaO_6$ (λ = 1.54 Å). Scattering from an empty sample can has been subtracted from these data. The magenta ticks represent the Bragg positions of the $P4_2/n$ double double perovskite phase.

Table 1: Structural parameters for $CaMnFeTaO_6$ from the 300 K neutron Rietveld fit with derived bond distances (Å) below. Residuals are: R_p = 4.44%, R_{wp}= 5.59%, R_{Bragg} = 4.52%, R_F= 3.01%, and χ^2= 2.37.

Atom*	*x*	*y*	*z*	B_{iso} (Å²)	occ.
Ca	0.250	0.750	0.776(1)	1.33(15)	1
A1 (Mn/Fe)	0.750	0.750	0.7500	0.65(3)	0.88/ 0.12(4)
A2 (Mn/Fe)	0.250	0.250	0.7500	0.65	0.76/ 0.24(1)
B1 (Fe/Ta)	0.000	0.500	0.5000	0.65	0.82/ 0.18(3)
B2 (Ta/Fe)	0.000	0.000	0.5000	0.65	0.82/ 0.18
O1	-0.051(1)	0.563(1)	0.249(2)	0.58(4)	1
O2	-0.242(2)	-0.047(1)	0.565(1)	0.58	1
O3	-0.252(3)	0.057(1)	-0.036(1)	0.58	1

Ca - O1	2.728(9) x 2	B1 – O1	2.026(15) x 2
Ca - O1	2.856(9) x 2	B1 – O2	2.073(13) x 2
Ca - O2	2.592(12) x 2	B1 – O3	2.005(7) x 2
Ca – O3	2.490(5) x 2	**<B1 – O>**	2.034(11)
Ca – O3	2.363(15) x 2	B2 – O1	2.011(15) x 2
<Ca – O>	2.606(10)	B2 – O2	1.961(13) x 2
A1 – O1	2.101(9) x 4	B2 – O3	1.975(7) x 2
A2 – O2	2.112(6) x 4	**<B2 – O>**	1.983(11)

*Wyckoff sites are Ca 4e; A1 2a; A2 2b; B1 4c; B2 4d; O1,O2,O3 8g.

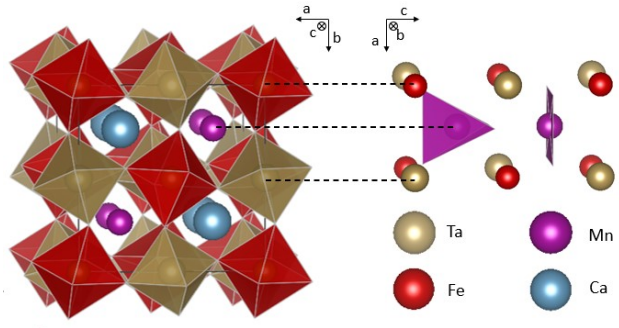

Figure 2: Structure of $CaMnFeTaO_6$ in space group $P4_2/n$ along with the arrangement of tetrahedral and square planar Mn^{2+} coordination sites within the A-site columns.

Refined oxygen coordinates enable precise bond distances and angles to be calculated. Bond Valence Sum (BVS) calculations[19] using the distances shown in Table 1 give values of 1.80, 1.46, 1.31, 2.34 and 4.16 for Ca, A1, A2, B1 and B2 sites respectively. These are consistent with the ideal formula $Ca^{2+}Mn^{2+}Fe^{3+}Ta^{5+}O_6$ but values for the transition metals are low reflecting the substantial disorder at their sites. Ca sits in a large 10-fold site and the bond lengths shown are in good agreement with values from other double double perovskites.[12,13,14] Bond angles of Fe-O1-Ta, along the *z*-axis, and Fe-O2-Ta and Fe-O3-Ta in the *xy* plane are 144.3(5), 144.4(3) and 149.7(3)°, which correspond to $B/B'O_6$ octahedra tilt angles of 17.9(3), 17.8(2), and 15.2(2)° respectively. The $P4_2/n$ double double perovskite structure is stabilised by these substantial tilts which create the distinct 10-coordinate Ca and 4-coordinate Mn A-site columns, as seen in Figure 2. The values for $CaMnFeTaO_6$ lie within the range of 15 to 20° octahedral

tilts reported from an analysis of structural evolution in the $MnRMnSbO_6$ series.[10]

The magnetic susceptibility against temperature plot for $CaMnFeTaO_6$ in Fig. 3a reveals paramagnetic behavior at high temperatures. A fit of the Curie-Weiss equation to inverse susceptibility above 150 K gave an effective paramagnetic moment of μ_{eff} = 6.71 μ_B per formula unit (f.u.) and a Weiss temperature of θ = -72 K. The moment is smaller than the theoretical spin-only value for $CaMnFeTaO_6$ of μ_{eff} = 8.37 μ_B $f.u^{-1}$. This may reflect the off-stoichiometry observed from the cation site refinement, and also suggests that higher temperature data would be needed to obtain a more accurate estimate of μ_{eff}. The negative Weiss temperature indicates that dominant spin-spin couplings are antiferromagnetic, consistent with the antiparallel, ferrimagnetic couplings of A and B site spins observed in other double double perovskites. Two apparent magnetic transitions are observed at low temperatures. A discontinuity as susceptibility deviates away from Curie-Weiss behavior is observed at T_{m1} = 51 K, and a susceptibility maximum below which zero field cooled (ZFC) and field cooled (FC) data diverge is seen at T_{m2} = 20 K.

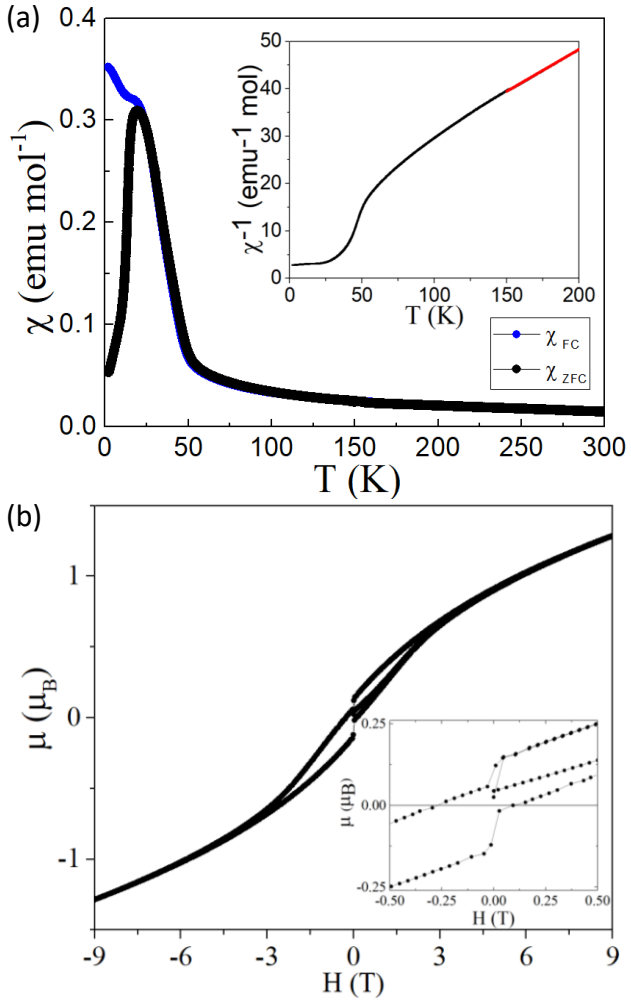

Figure 3: (a) Magnetic susceptibility (ZFC and FC data) and inverse magnetic susceptibility (FC, inset) for $CaMnFeTaO_6$ measured at a field of 0.1 T. Red line shows the Curie-Weiss fit. (b) Hysteresis loop of $CaMnFeTaO_6$ at 2 K with low field data expanded in the inset.

The magnetization-field (*M-H*) loop at 2 K in Fig. 3b has a sharp hysteretic magnetisation feature at fields below 0.1 T (shown in the inset). This is most likely due to traces of a magnetic impurity such as $(Fe,Mn)_3O_4$ spinel, below the limit of detection in our diffraction experiments. The *M-H* variation otherwise evidences superparamagnetic or glassy rather than ferromagnetic behavior, as *M*(*H*) shows continuous curvature with very little hysteresis and does not saturate even at the highest field of 9 T.

Further D20 neutron diffraction scans using wavelength λ = 2.41 Å were taken at 30 K and 1.5 K to detect any changes in neutron scattering below T_{m1} = 51 K and T_{m2} = 20 K respectively. The low angle scattering region where magnetic peaks are expected is shown in Fig. 4a. Previously investigated double double perovskites[10-14] have all had low temperature spin orders with propagation vector ***k*** = [0 0 0] giving magnetic diffraction contributions at nuclear peak positions. However, no magnetic peaks are observed for $CaMnFeTaO_6$ from ***k*** = [0 0 0] or other vectors at either 30 or 1.5 K. An additional magnetic diffraction peak is observed at 2θ = 28.5°, but this is the intense (½ ½ ½) diffraction peak from a trace of MnO impurity (consistent with the Mn-poor composition of the double double perovskite phase) which orders antiferromagnetically below 120 K. Other additional features (sharp peak at 34°, broad signals at 41-44° and 53-56°) are spurious scattering from the instrument or sample environment. (These were also seen for other samples studied during the same neutron experiment, and so are not from the $CaMnFeTaO_6$ sample.)

Rietveld fits to the neutron diffractions scans at 1.5 and 30 K were carried out using the nuclear structure model from the 300 K refinement (Table 1). The magnetic MnO peak was Le Bail fitted as the nuclear peaks from this phase are not visible, and the spurious scattering regions were excluded. A magnetic structure fit was attempted using a ***k*** = [0 0 0] ferrimagnetic model, with A1 and A2 site Mn spins antiparallel to those from Fe at B1 sites. However, this made no visible difference or statistical improvement to the profile fitting, and magnetic moments were within their estimated standard deviations. We therefore conclude that any long-range ordered magnetic moments in $CaMnFeTaO_6$ are below the effective limit of ~0.5 μ_B for their detection in these neutron diffraction experiments. Formation of such small, long range ordered moments is unlikely given that ideal ordered moments of 5 μ_B are expected for high spin S = 5/2 Fe^{3+} and Mn^{2+} cations. The 1.5 K fit is shown in Fig. 4b. Refined lattice parameters were a = 7.662(1) and c = 7.661(1), and a = 7.664(1) and c = 7.663(2) Å, at 1.5 K and 30 K respectively.

The absence of magnetic peaks in the neutron diffraction profiles demonstrates that the transitions observed in the magnetisation data correspond to short range spin orders. The magnetisation peak at T_{m2} = 20 K is typical of a spin glass, however, spin glasses do not usually also show a Curie-like transition as seen for $CaMnFeTaO_6$ at T_{m1} = 51 K. A likely

explanation is that superparamagnetic clusters of ferrimagnetically-aligned spins are formed below the Curie-like transition at T_{m1}, and that these freeze into a cluster spin glass at T_{m2}. The correlation length for the spin ordering within clusters is too short for any magnetic diffraction peaks to be seen in the neutron scattering data, and there is no long-range correlation between frozen cluster spin directions. Any diffuse magnetic scatter is not distinguished from other background contributions in our low temperature data (Fig. 4a).

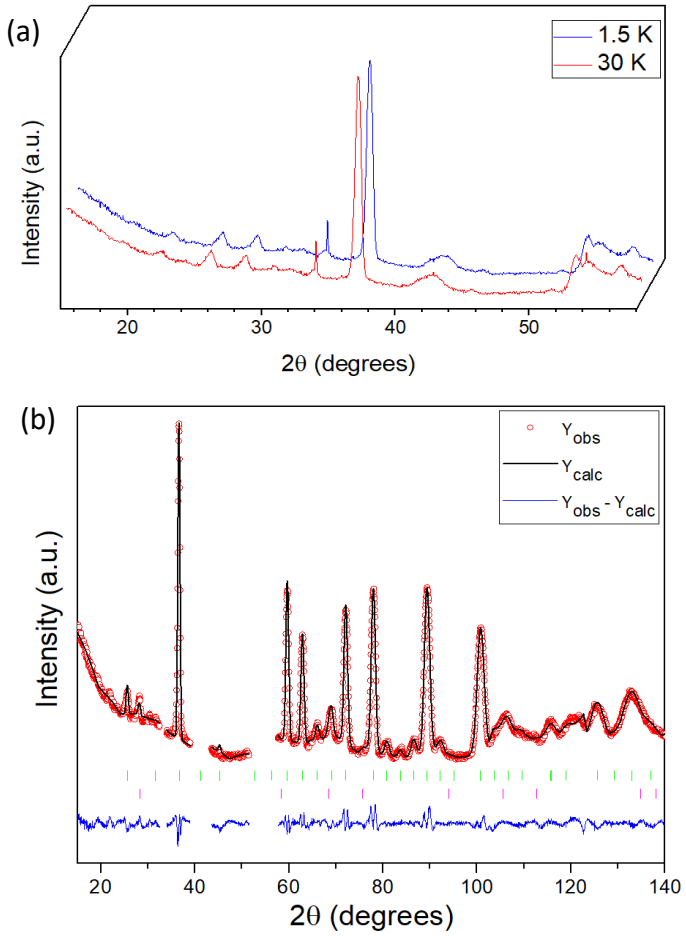

Figure 4: (a) Comparison of low angle λ = 2.41 Å neutron diffraction patterns of $CaMnFeTaO_6$ at 1.5 and 30 K. (b) Rietveld fit to the 1.5 K profile. $CaMnFeTaO_6$ peak positions are shown by the green ticks, and those from the magnetic MnO impurity phase, with Le Bail fitted intensities are magenta.

AC magnetisation data at varying frequencies ω were recorded to explore the proposed cluster spin glass ground state (Fig. 5). The susceptibility peak for $CaMnFeTaO_6$ shows an increase with frequency confirming that it corresponds to a spin freezing transition at $T_f = T_{m2}$. The $\Delta T_f = 0.23$ K increase over the observed frequency range corresponds to a shift per frequency decade $\phi = \Delta T_f/(T_f \Delta \log\omega) = 0.006$. This is below the typical range of 0.01 to 0.1 for standard spin glasses, but is in good agreement with values for reported cluster spin glass materials; $\phi = 0.005$ for U_2IrSi_3 and $\phi = 0.002$ for the oxygen deficient perovskite $BaBi_{0.28}Co_{0.72}O_{2.2}$.[20] The variation of T_f can be fitted by the Vogel-Fulcher function $\omega = \omega_0 \exp[-E_a/k_B(T_f - T_0)]$ as shown in the inset to Fig. 5. However, attempts to fit the ideal glass temperature T_0, characteristic frequency ω_0 and activation energy E_a simultaneously gave highly correlated values. E_a/k_B is typically in the range 0.2-2T_f for cluster spin glasses but 2-10T_f for conventional spin glasses. Fixing $E_a/k_B = 0.5T_f$ = 13 K gave ω_0 = 1.5(11) GHz and T_0 = 25.3(1) K for $CaMnFeTaO_6$, comparable to $E_a/k_B = 0.24T_f$ = 6(1) K fitted at fixed ω_0 = 1 GHz for the cluster spin glass $BaBi_{0.28}Co_{0.72}O_{2.2}$ which has a similar T_0 = 25.0(1) K.[20]

Other features of cluster spin glasses apparent in our susceptibility measurements for $CaMnFeTaO_6$ are strong suppression of T_f by applied magnetic field and slow relaxation dynamics. T_f changes by 23% from 26 K at zero field in the AC data to 20 K at 0.1 T in the DC measurement (Fig. 3a). A 50% reduction of T_f over the same field change was observed in $BaBi_{0.28}Co_{0.72}O_{2.2}$,[20] and a 36% suppression was reported for the cation disordered perovskite cluster spin glass $SrMn_{0.5}Ti_{0.5}O_3$ (Sr_2MnTiO_6) as field increased from 0.01 to 1 T.[21] Slow relaxation dynamics in $CaMnFeTaO_6$ are evidenced by the changes of slope seen in the AC susceptibility data of Fig. 5 at 20 and 30 K, where the cooling rate was changed by a factor of two, but were not explored more systematically.

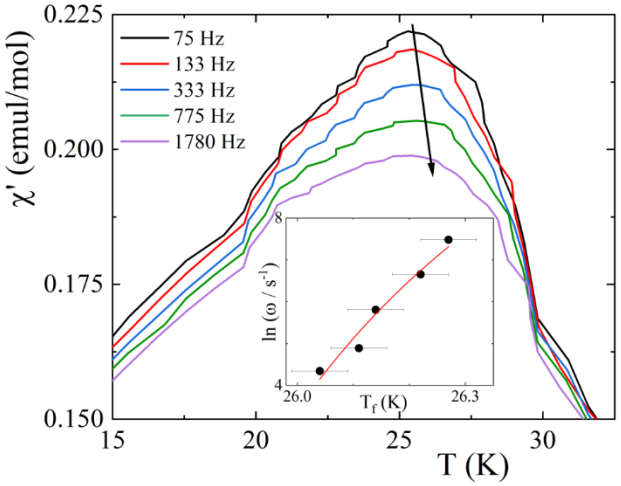

Figure 5: Real part of the AC magnetic susceptibility data for $CaMnFeTaO_6$, collected at the frequencies ω shown while cooling from 70 to 2 K in steps of 0.5 K between 30 and 20 K and of 1 K outside this range. Each step was recorded for 1 min in zero applied field with an AC drive field of 16 Oe. Inset shows Vogel-Fulcher fit to the T_f values.

Spin glass ground states are found in many doped or disordered perovskite oxides such as and sometimes result from freezing of magnetic polarons, ferromagnetic clusters of up to ~100 spins, e.g. in $La_{1-x}Sr_xCoO_3$.[22] The observation of a Curie-like magnetisation discontinuity in $CaMnFeTaO_6$

suggests that the magnetic clusters are much larger, comprising up to ~10^6 spins in the superparamagnetic regime. Cluster spin glass behaviour has been reported in $BaBi_{0.28}Co_{0.72}O_{2.2}$ as above[20] and several disordered double perovskites such as $Sr_2Mn_{1-x}Fe_xMoO_6$, where Mn and Fe are randomised at one of the B-sites,[23] and Sr_2FeCoO_6 [24] and Sr_2MnTiO_6,[20] where B-cations are fully disordered. Observation of thermoremanent magnetization with slow relaxation dynamics and other memory effects were used to evidence the cluster spin glass state in the latter material, and similar experiments could be used to further characterise $CaMnFeTaO_6$.

The formation of a glassy magnetic ground state in the double double perovskite $CaMnFeTaO_6$ reflects both the dilution effect of introducing non-magnetic Ta^{5+} into the B-cation network, and the effect of cation disorder at transition metal sites. Neither factor appears sufficient by itself; $MnLaMnSbO_6$ has the same concentration of S = 5/2 cations as $CaMnFeTaO_6$ but has long range ferrimagnetic order below T_c = 48 K; and levels of cation disorder and non-stoichiometry observed in $CaMnCoReO_6$ ($CaMn_{0.7}Co_{1.3}ReO_6$) and $CaMnNiReO_6$ ($CaMn_{1.2}Ni_{0.8}ReO_6$) are similar to those in $CaMnFeTaO_6$ ($CaMn_{0.8}Fe_{1.2}TaO_6$) but the former materials based on S = 1/2 Re^{6+} have long range spin orders below T_c = 188 and 152 K respectively. Hence both the presence of non-magnetic Ta^{5+} and the observed 18% inversion disorder in $CaMnFeTaO_6$ are important to disruption of the B-site spin order. The substitution of 12-24% Fe^{2+} for Mn^{2+} at the A1 and A2 sites is also likely to be disruptive as M-O-M superexchange interactions between the M = Mn^{2+} and Fe^{3+} d^5 cations are expected to be antiferromagnetic whereas M-O-Fe^{2+} superexchange interactions can be ferromagnetic.[25] The effects of both Fe^{3+}/Ta^{5+} and Fe^{2+}/Mn^{2+} cation disorders on the complex network of exchange interactions between A1, A2, B1, (and B2) sites evidently creates enough randomness to disrupt long-range spin order in $CaMnFeTaO_6$ so that only short-range magnetic cluster glass behavior is observed down to 1.5 K.

CONCLUSIONS

$CaMnFeTaO_6$ extends the range of magnetic ground states observed in the *P4₂/n* family of double double perovskites. Long range ferro-, ferri-, and antiferro- magnetic orders have all previously been reported, but $CaMnFeTaO_6$ has a cluster spin glass ground state without long range magnetic order. This opens possibilities for further glassy or even quantum spin liquid ground states to be discovered through chemical substitution and disorder tuning within this flexible structure type.

ACKNOWLEDGMENT

We acknowledge EPSRC for financial support and STFC for provision of beamline at the Institut Laue-Langevin.

REFERENCES

1 Vasala, S.; Karppinen, M. $A_2B'B''O_6$ Perovskites: A Review. *Prog. Solid State Chem.* **2015**, *43*, 1– 36.

2 King, G.; Woodward, P. M. Cation ordering in perovskites. *J. Mater. Chem.* **2010**, *20*, 5785– 5796.

3 Kobayashi, K. I.; Kimura, T.; Sawada, H.; Terakura, K.; Tokura, Y. Room-Temperature Magnetoresistance in an Oxide Material with an Ordered Double-Perovskite Structure. *Nature* **1998**, *395*, 677-680.

4 Serrate, D.; De Teresa, J. M.; Ibarra, M. R. Double Perovskites with Ferromagnetism above Room Temperature. *J. Phys.: Condens. Matter* **2007**, *19*, 023201.

5 Li, M.-R.; Retuerto, M.; Deng, Z.; Stephens, P. W.; Croft, M.; Huang, Q.; Wu, H.; Deng, X.; Kotliar, G.; Sanchez-Benítez, J.; et al, M. Giant magnetoresistance in the half-metallic double-perovskite ferrimagnet Mn_2FeReO_6. *Angew. Chem., Int. Ed.* **2015**, *54*, 12069−12073.

6 Arevalo-Lopez, A. M.; McNally, G. M.; Attfield, J. P. Large magnetization and frustration switching of magnetoresistance in the double-perovskite ferrimagnet Mn_2FeReO_6. *Angew. Chem., Int. Ed.* **2015**, *54*, 12074−12077.

7 Arévalo-López, A. M.; Stegemann, F.; Attfield, J. P. Competing Antiferromagnetic Orders in the Double Perovskite Mn_2MnReO_6 (Mn_3ReO_6). *Chem. Commun.* **2016**, *52*, 5558-5560.

8 Frank, C. E.; McCabe, E. E.; Orlandi, F.; Manuel, P.; Tan, X.; Deng, Z.; Croft, M.; Cascos, V.; Emge, T.; Feng, H. L.; et al. Mn_2CoReO_6: a robust multi-sublattice antiferromagnetic perovskite with small A-site cations. *Chem. Commun.* **2019**, *55*, 3331−3334.

9 Solana-Madruga, E.; Alharbi, K. N.; Herz, M.; Manuel, P.; Attfield, J. P. 2020, Unconventional magnetism in the high pressure 'all transition metal' double perovskite Mn_2NiReO_6. *Chem. Commun.*, **2020**, *56*, 12574-12577.

10 Solana-Madruga, E.; Árévalo-López, Á. M.; Dos Santos-García, A. J.; Urones-Garrote, E.; Ávila-Brande, D.; Sáez-Puche, R.; Attfield, J. P. Double Double Cation Order in the High-Pressure Perovskites $MnRMnSbO_6$. *Angew. Chem., Int. Ed.* **2016**, *55*, 9340–9344.

11 Solana-Madruga, E.; Arevalo-Lopez, A. M.; Dos Santos-Garcia, A. J.; Ritter, C.; Cascales, C.; Saez-Puche, R.; Attfield, J. P. Anisotropic magnetic structures of the

$MnRMnSbO_6$ high-pressure doubly ordered perovskites. *Phys. Rev. B*, **2018**, *97*, 134408.

12 McNally, G. M.; Arevalo-Lopez, A. M.; Kearins, P.; Orlandi, F.; Manuel, P.; Attfield, J. P. Complex Ferrimagnetism and Magnetoresistance Switching in Ca-Based Double Double and Triple Double Perovskites. *Chem. Mater.*, **2017**, *29*, 8870–8874.

13 McNally, G. M.; Arévalo-López, Á. M.; Guillou, F.; Manuel, P.; Attfield, J. P. Evolution of cation and spin orders in the double-double-double perovskite series $Ca_xMn_{2-x}FeReO_6$. *Phys. Rev. Materials*, **2020**, *4*, 064408.

14 Solana-Madruga, E.; Sun, Y.; Arévalo-López, Á. M.; Attfield, J. P. Ferri-and ferro-magnetism in $CaMnMReO_6$ double double perovskites of late transition metals M= Co and Ni. *Chem. Commun.*, **2019**, *55*, 2605–2608.

15 Rodriguez-Carvajal, J. Recent advances in magnetic structure determination by neutron powder diffraction. *Physica B*, **1993**, *192*, 55–69.

16 Sears, V. F. Neutron scattering lengths and cross sections. *Neutron News*, **1992**, *3*, 26–37.

17 Aranda, M. A. G.; Sinclair, D. C.; Attfield, J. P. Cation distribution in the superconducting Tl,Pb-1223 phase ("$Tl_{0.5}Pb_{0.5}Sr_2Ca_2Cu_3O_9$") from resonant synchrotron powder X-ray diffraction. *Physica C* **1994**, *221*, 304-310.

18 Tsujimoto, Y.; Tassel, C.; Hayashi, N.; Watanabe, T.; Kageyama, H.; Yoshimura, K.; Takano, M.; Ceretti, M.; Ritter, C.; Paulus, W. Infinite-layer iron oxide with a square-planar coordination. *Nature*, **2007**, *450*, 1062–1065.

19 Brown, I. D. Recent Developments in the Methods and Applications of the Bond Valence Model. *Chem. Rev.* **2009**, *109*, 6858−6919.

20 Klimczuk, T.; Zandbergen, H. W.; Huang, Q.; McQueen, T. M.; Ronning, F.; Kusz, B.; Thompson, J. D.; Cava, R. J. Cluster-glass behavior of a highly oxygen deficient perovskite, $BaBi_{0.28}Co_{0.72}O_{2.2}$. *J. Phys.: Condens. Matter* **2009**, *21*, 105801.

21 Sharma, S.; Yadav, P.; Sau, T.; Yanda, P.; Baker, P. J.; da Silva, I.; Sundaresan, A.; Lalla, N. P. Evidence of a cluster spin-glass state in B-site disordered perovskite $SrTi_{0.5}Mn_{0.5}O_3$. *J. Magnetism Magnetic Materials*, **2019**, *492*, 165671.

22 Anil Kumar, P.; Nag, A.; Mathieu, R.; Das, R.; Ray, S.; Nordblad, P.; Hossain, A.; Cherian, D. ; Venero, D. A.; DeBeer-Schmitt, L.; et al. Magnetic polarons and spin-glass behavior in insulating $La_{1-x}Sr_xCoO_3$ (x = 0.125 and 0.15). *Phys. Rev. Research*, **2020**, *2*, 043344.

23 Poddar, A.; Mazumdar, C. Magnetic frustration effect in Mn rich $Sr_2Mn_{1-x}Fe_xMoO_6$ system. *J. Appl. Phys.*, **2009**, *106*, 093908.

24 Pradheesh, R.; Nair, H. S.; Kumar, C. M. N.; Lamsal, J.; Nirmala, R.; Santhosh, P. N.; Yelon, W. B.; Malik, S. K.; Sankaranarayanan, V.; Sethupathi, K. Observation of spin glass state in weakly ferromagnetic Sr_2FeCoO_6 double perovskite *J. Appl. Phys.*, **2012**, *111*, 053905.

25 Goodenough, J. B.. Magnetism and the Chemical Bond, New York: Wiley, **1963**.

TOC graphic